Research Square

Preprints are preliminary reports that have not undergone peer review.
They should not be considered conclusive, used to inform clinical practice,
or referenced by the media as validated information.

Receiver Sensitivity Limits, Forward Error Correction, and Adaptive Beam Divergence for Space Laser Links: When Does Adapting the Beam Pay Off?

SATHISHA R N

sathisharyan@sit.ac.in

Siddaganga Institute of Technology https://orcid.org/0000-0001-8031-7611

Research Article

Keywords: free-space optical communication, inter-satellite links, receiver sensitivity, quantum limit, forward error correction, low-density parity-check, pointing jitter, adaptive divergence, liquid lens, outage probability

Posted Date: November 12th, 2026

DOI: https://doi.org/10.21203/rs.3.rs-11706630/v1

License: This work is licensed under a Creative Commons Attribution 4.0 International License.
Read Full License

Additional Declarations: The authors declare no competing interests.

Receiver Sensitivity Limits, Forward Error Correction, and Adaptive Beam Divergence for Space Laser Links: When Does Adapting the Beam Pay Off?

Sathisha R. N.
Department of Electronics and Telecommunication Engineering
Siddaganga Institute of Technology, Tumakuru 572103, Karnataka, India
Email: satisharyan@gmail.com ORCID: 0000-0001-8031-7611

November 2026

Abstract

Space laser terminals designed for low-Earth-orbit (LEO) to geostationary (GEO) data relay must establish reliable links at weak received optical powers while the spacecraft platform microvibrates with pointing jitter of several microradians. We examine four 1550 nm receiver architectures—PIN, avalanche photodiode (APD), optically pre-amplified on-off keying (OOK), and optically pre-amplified balanced differential phase-shift keying (DPSK)—referenced directly against the fundamental quantum limit and standard Forward Error Correction (FEC) operating bounds. An optically pre-amplified DPSK receiver satisfies -55 dBm sensitivity at an uncoded bit error rate (BER) of 10^{-6} only up to approximately 600 Mb/s. At 10 Gb/s, an incident power of -55 dBm corresponds to only 2.47 photons/bit, which falls well below the fundamental 13.11 photons/bit binary quantum limit; consequently, a flat -55 dBm requirement across multi-gigabit bands is physically infeasible above 1.88 Gb/s uncoded and above 3.5 Gb/s even when augmented by soft-decision low-density parity-check (LDPC) coding. We subsequently evaluate Gaussian beam divergence optimization under Rayleigh-distributed pointing jitter. For a fixed data rate, we prove analytically that the outage-optimal beam divergence θ^* is invariant to the pointing jitter magnitude σ, occurring uniquely when the on-axis peak received power exceeds the receiver sensitivity by exactly e (4.34 dB margin). Conversely, for a rate-adaptive link, optimal divergence scales strictly linearly with jitter ($\theta_{\text{opt}} = \sigma\sqrt{-4\ln P_{\text{out}}}$). In trans-atmospheric downlinks, Gamma-Gamma scintillation reintroduces jitter dependence even at a fixed data rate. A 60-second time-domain simulation of a LEO–GEO relay terminal driven by realistic attitude disturbance profiles demonstrates that a four-state liquid-lens divergence controller recovers 95% more throughput during mechanical disturbances than an optimal static beam. Adaptive divergence is therefore justified for rate-adaptive terminals and atmospheric paths, but provides negligible advantage for fixed-rate inter-satellite links.

Keywords: Free-space optical communication, inter-satellite links, receiver sensitivity, quantum limit, forward error correction, low-density parity-check, pointing jitter, beam divergence, liquid lens, outage probability.

1 Introduction

Laser communication terminals are now operational across multiple orbital regimes. Demonstrations such as the European Data Relay System (EDRS) have established routine 1.8 Gb/s relay services across $45{,}000$ km inter-satellite baselines [1, 2]. Upcoming space relay, Earth

Preprint submitted to IEEE for possible publication. Copyright may be transferred without notice.

observation, and crewed orbital programs confront two foundational physical design constraints: establishing the achievable photon-efficiency boundaries of high-speed optical receivers, and selecting the optimal transmit beam divergence in the presence of satellite microvibrations and attitude tracking jitter [3].

Receiver sensitivity in space acquisition programs is frequently formulated as a uniform power threshold across broad transmission bandwidths. For example, recent agency research challenges specify an ultra-sensitive optical receiver capable of detecting power levels below -55 dBm across continuous data rates from 50 Mb/s to 10 Gb/s at BER $\leq 10^{-6}$ [3]. However, fundamental quantum and information-theoretic principles demonstrate that physical sensitivity scales primarily in photons per bit rather than constant power [4]. As transmission rates increase into the multi-gigabit regime, invariant power specifications eventually violate quantum limits.

Simultaneously, transmit beam divergence governs the trade-off between on-axis optical power density and tolerance to pointing misalignment. Chen and Gardner established analytical foundations for optimal transceiver antenna gains under pointing error uncertainty [5]. Toyoshima *et al.* optimized the beam divergence-to-jitter ratio to minimize average bit error rate [6]. Farid and Hranilovic evaluated outage capacity under combined pointing error and atmospheric turbulence [7], while Xue *et al.* optimized beam divergence for link reliability [8]. Arnon and Kopeika investigated dynamic beam broadening to suppress satellite vibration degradation [9].

Recent experimental advances in variable-focus liquid lenses (electrowetting and fluidic elastomeric architectures) offer rapid, non-mechanical divergence adaptability [10, 11]. Because liquid lenses avoid mechanical translation stages and have survived preliminary space-qualification testing [12], they represent a practical solution for dynamic spatial beam control.

Despite these advances, the literature lacks a unified analytical criterion defining exactly *when* adaptive divergence provides an operational advantage over an optimal static beam. The answer depends heavily on the optimization metric: average-BER optimization assumes jitter that fluctuates rapidly across individual codewords [6], whereas outage probability governs slow, correlated mechanical microvibrations—such as reaction wheel zero-crossings, antenna slews, and thruster firings [1].

This paper makes four specific contributions:

1. A quantum-limit-benchmarked sensitivity analysis across PIN, APD, optically pre-amplified OOK, and pre-amplified balanced DPSK receivers, demonstrating that -55 dBm is physically impossible above 1.88 Gb/s and constrained to ≤ 595 Mb/s in practical pre-amplified DPSK architectures.

2. A closed-form analytical proof demonstrating that for fixed-rate space links under Rayleigh pointing jitter, the outage-optimal beam divergence is invariant to platform jitter standard deviation σ, occurring uniquely at $P_{\text{pk}} = e \cdot S$ (4.34 dB margin).

3. An analytical formulation for rate-adaptive optical links showing that optimal divergence scales strictly linearly with jitter ($\theta_{\text{opt}} \propto \sigma$), with atmospheric Gamma-Gamma turbulence restoring jitter sensitivity even in fixed-rate regimes.

4. A 60-second time-domain dynamic simulation of a LEO–GEO relay terminal driven by an autoregressive disturbance profile, demonstrating that a four-state liquid-lens controller achieves a 95% throughput enhancement during platform disturbances compared to optimal static beams.

Preprint submitted to IEEE for possible publication. Copyright may be transferred without notice.

2 System Architecture and Physical Parameters

Table 1 compiles the baseline system parameters employed across our analytical derivations and numerical simulations.

Table 1: System Simulation and Physical Baseline Parameters

Parameter	Symbol	Value
Operating Wavelength	λ	1550 nm
Transmitter Laser Power	P_t	1.0 W (30 dBm)
Terminal Optics Losses (Tx / Rx)	L_{opt}	3.0 dB / 3.0 dB
Fiber Coupling Loss	L_{fiber}	2.0 dB
Optical Preamplifier Gain	G	30.0 dB
Preamplifier Noise Figure	NF	4.5 dB
Optical Filter Bandwidth	B_o	12.5 GHz (0.1 nm)
Photodetector Quantum Efficiency	η_q	0.80 ($\mathcal{R} \approx 1.0$ A/W)
Total Junction Capacitance	C_T	0.3 pF
Transimpedance Noise Figure	F_n	2.0
APD Ionization Ratio	k_A	0.45
Maximum APD Optimal Gain	M_{max}	40
DPSK Implementation Penalty	η_{pen}	1.5 dB
Jitter Autoregressive Bandwidth	f_c	50 Hz

2.1 Receiver Formulations

Photocurrent detection for On-Off Keying (OOK) is evaluated via the Gaussian approximation:

$$\text{BER} = \frac{1}{2}\text{erfc}\left(\frac{Q}{\sqrt{2}}\right), \qquad Q = \frac{I_1 - I_0}{\sigma_1 + \sigma_0}, \tag{1}$$

where I_1 and I_0 denote the signal photocurrents for binary symbols "1" and "0", and σ_1, σ_0 represent the associated noise standard deviations.

For a PIN photodiode receiver, circuit thermal noise dominates. Load matching yields $R_L = [2\pi C_T B_e]^{-1}$, with electrical bandwidth $B_e = 0.7R_b$. Consequently, thermal noise variance $\sigma^2_{\text{th}} = (4k_BTF_n/R_L)B_e$ scales quadratically with bit rate ($\propto R_b^2$).

For an avalanche photodiode (APD), avalanche multiplication gain M introduces excess noise according to $F(M) = k_AM + (1 - k_A)(2 - 1/M)$. At every incident power level, M is optimized numerically within $1 \leq M \leq 40$ to balance shot-noise multiplication against thermal noise.

For an optically pre-amplified OOK receiver, amplified spontaneous emission (ASE) from the erbium-doped fiber amplifier (EDFA) dominates. The single-polarization spectral density of ASE is $S_{\text{sp}} = n_{\text{sp}}h\nu(G - 1)$, where $n_{\text{sp}} = (G \cdot \text{NF} - 1)/[2(G - 1)]$. Taking into account coupling loss prior to amplification ($P_{\text{in}} = P_{\text{rx}}L_{\text{fiber}}$), the signal-spontaneous and spontaneous-spontaneous beat noise components are:

$$\sigma^2_{s\text{-sp}} = 4\mathcal{R}^2GP_{\text{in}}S_{\text{sp}}B_e, \qquad \sigma^2_{\text{sp-sp}} = 2\mathcal{R}^2S^2_{\text{sp}}(2B_o - B_e)B_e. \tag{2}$$

For pre-amplified balanced DPSK detection, optical delay-line demodulation cancels spontaneous-spontaneous beat noise, leaving receiver sensitivity governed by the number of incident photons per bit $N_p = (P_{\text{in}}/R_b)/(h\nu)$:

$$\text{BER}_{\text{DPSK}} = \frac{1}{2}\exp\left(-\frac{N_p}{n_{\text{sp}}\eta_{\text{pen}}}\right). \tag{3}$$

Preprint submitted to IEEE for possible publication. Copyright may be transferred without notice.

Under ideal amplification ($n_{\text{sp}} = 1$) and zero implementation penalty ($\eta_{\text{pen}} = 1$), this reduces to the fundamental binary DPSK quantum limit:

$$\text{BER}_{\text{QL}} = \frac{1}{2}\exp(-N_p), \tag{4}$$

requiring exactly $N_p = 13.11$ photons/bit to satisfy BER $= 10^{-6}$.

2.2 Forward Error Correction (FEC) and Pre-FEC Thresholds

Operational space laser links do not operate uncoded at BER $= 10^{-6}$. Instead, spaceborne optical transceivers (such as the DVB-S2/S2X and CCSDS 141.0-B-1 optical telecommand standards) incorporate low-density parity-check (LDPC) or hard-decision staircase codes. Modern space-grade soft-decision LDPC codes operate with an uncoded pre-FEC bit error threshold of $\text{BER}_{\text{pre}} \approx 10^{-2}$ to 10^{-3}, delivering a quasi-error-free post-FEC BER $\leq 10^{-12}$ with a net coding gain (NCG) of 6.0 to 9.2 dB.

At an uncoded threshold of $\text{BER}_{\text{pre}} = 10^{-3}$, the required quantum limit for binary DPSK reduces from $N_p = 13.11$ photons/bit to:

$$N_{p,\text{pre}} = -\ln(2 \cdot 10^{-3}) \approx 6.21 \text{ photons/bit}. \tag{5}$$

Incorporating our realistic implementation penalty ($\eta_{\text{pen}} = 1.5$ dB), amplifier spontaneous emission factor ($n_{\text{sp}} = 1.41$), and fiber coupling loss ($L_{\text{fiber}} = 2.0$ dB), the pre-FEC sensitivity requirement of pre-amplified DPSK evaluates to $N_{p,\text{FEC}} \approx 19.5$ photons/bit.

While FEC shifts the operational sensitivity curve downward by 6–9 dB across all bit rates, it does *not* alter the fundamental physical conclusion: at 10 Gb/s, an optical input power of -55 dBm delivers only 2.47 photons/bit. Because 2.47 photons/bit remains strictly below the pre-FEC quantum limit (6.21 photons/bit), a -55 dBm link closure at 10 Gb/s remains physically impossible even in the presence of state-of-the-art soft-decision FEC. Furthermore, because FEC scales the receiver threshold S by a uniform constant gain factor G_{code}, the mathematical derivation of Theorem 1 remains invariant.

2.3 Gaussian Beam Propagation and Pointing Jitter

A fundamental Gaussian beam with $1/e^2$ beam waist half-angle divergence θ delivers on-axis peak received power:

$$P_{\text{pk}}(\theta) = \frac{K}{\theta^2}, \qquad K = P_t \eta_{\text{opt}} \left(\frac{2A_r}{\pi L^2}\right), \tag{6}$$

where $A_r = \pi D_r^2/4$ is the receiver aperture area, L is the orbital link distance, and η_{opt} accounts for lumped transceiver losses. In the presence of a radial pointing misalignment angle θ_e, intercepted optical power degrades exponentially:

$$P_{\text{rx}}(\theta, \theta_e) = \frac{K}{\theta^2}\exp\left(-\frac{2\theta_e^2}{\theta^2}\right). \tag{7}$$

Assuming orthogonal azimuth (θ_x) and elevation (θ_y) errors are independent zero-mean Gaussian random variables $\mathcal{N}(0, \sigma^2)$, the radial deviation $\theta_e = \sqrt{\theta_x^2 + \theta_y^2}$ follows a Rayleigh distribution:

$$f_{\theta_e}(\theta_e) = \frac{\theta_e}{\sigma^2}\exp\left(-\frac{\theta_e^2}{2\sigma^2}\right), \qquad \theta_e \geq 0. \tag{8}$$

Temporal platform jitter is simulated as a continuous first-order autoregressive AR(1) process with a 50 Hz corner frequency, modeling residual attitude control tracking errors.

2.4 Atmospheric Scintillation Modeling

For ground downlink paths, irradiance fluctuations are modeled via the Gamma-Gamma distribution:

$$f_I(I) = \frac{2(\alpha\beta)^{(\alpha+\beta)/2}}{\Gamma(\alpha)\Gamma(\beta)} I^{\left(\frac{\alpha+\beta}{2}\right)-1} K_{\alpha-\beta}\left(2\sqrt{\alpha\beta I}\right), \tag{9}$$

where α and β represent effective large-scale and small-scale turbulent eddy parameters determined by the spherical-wave Rytov variance σ_R^2:

$$\alpha = \left[\exp\left(\frac{0.49\sigma_R^2}{(1+1.11\sigma_R^{12/5})^{7/6}}\right) - 1\right]^{-1}, \qquad \beta = \left[\exp\left(\frac{0.51\sigma_R^2}{(1+0.69\sigma_R^{12/5})^{5/6}}\right) - 1\right]^{-1}. \tag{10}$$

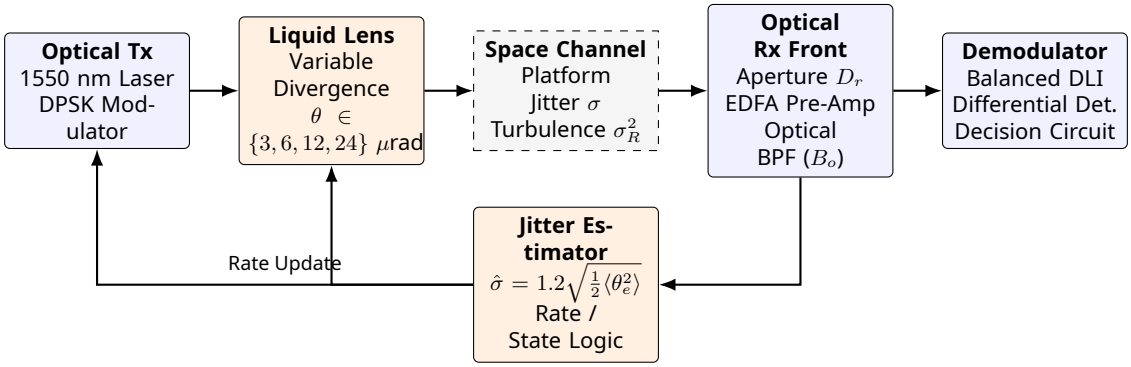


Figure 1: End-to-end space optical link architecture featuring adaptive liquid-lens divergence control, dynamic jitter estimation, and an optically pre-amplified balanced DPSK receiver front end.

3 Receiver Sensitivity Limits and the Quantum Barrier

Table 2 outlines the precise sensitivity figures across rates at a target BER $= 10^{-6}$. The pre-amplified DPSK receiver operates at a fixed photon efficiency of 41.3 photons/bit, placing it 5.0 dB above the quantum limit (2.0 dB fiber coupling loss, 1.5 dB demodulator penalty, and 1.5 dB amplifier excess noise). Pre-amplified OOK requires 115 to 381 photons/bit, constrained by spontaneous-spontaneous beat noise in the 12.5 GHz optical passband at lower rates. APD and PIN receivers require 572–875 photons/bit and $\approx 6{,}900$ photons/bit, respectively.

The fundamental physical constraint appears in the final row of Table 2. At 10 Gb/s, an optical power of -55 dBm (3.16×10^{-9} W) provides an energy of 3.16×10^{-19} J per bit. At $\lambda = 1550$ nm, photon energy is $h\nu = 1.28 \times 10^{-19}$ J, meaning that -55 dBm corresponds to only:

$$N_p = \frac{3.16 \times 10^{-19}\ \text{J}}{1.28 \times 10^{-19}\ \text{J}} \approx 2.47\ \text{photons/bit}. \tag{11}$$

Because the quantum limit for binary DPSK requires 13.11 photons/bit at BER $= 10^{-6}$, -55 dBm is physically impossible at 10 Gb/s. Even ideal coherent BPSK (providing a 3 dB sensitivity advantage) requires 6.55 photons/bit, bounding coherent sensitivity at 3.76 Gb/s.

Consequently, program specifications stipulating -55 dBm up to 10 Gb/s cannot be met by any physical receiver. Realistic specifications must define photon-efficiency bounds (≈ 40 photons/bit for pre-amplified DPSK) or scale sensitivity proportionally with data rate (e.g., -55 dBm at 500 Mb/s, transitioning to -43 dBm at 10 Gb/s).

Preprint submitted to IEEE for possible publication. Copyright may be transferred without notice.

Table 2: Receiver Sensitivity (P_{rx} in dBm) at BER $= 10^{-6}$

Bit Rate	PIN	APD	EDFA-OOK	EDFA-DPSK	Quantum Limit
50 Mb/s	-43.5	-52.5	-56.1	-65.8	-70.8
100 Mb/s	-40.5	-50.1	-54.2	-62.7	-67.7
250 Mb/s	-36.5	-46.7	-51.6	-58.8	-63.8
500 Mb/s	-33.5	-44.0	-49.4	-55.8	-60.8
1 Gb/s	-30.5	-41.1	-47.1	-52.7	-57.7
2.5 Gb/s	-26.5	-37.3	-43.8	-48.8	-53.8
5 Gb/s	-23.5	-34.3	-41.1	-45.8	-50.8
10 Gb/s	-20.5	-31.3	-38.3	-42.7	-47.7
Max Rate at -55 dBm	< 10 Mb/s	24 Mb/s	76 Mb/s	595 Mb/s	1.88 Gb/s

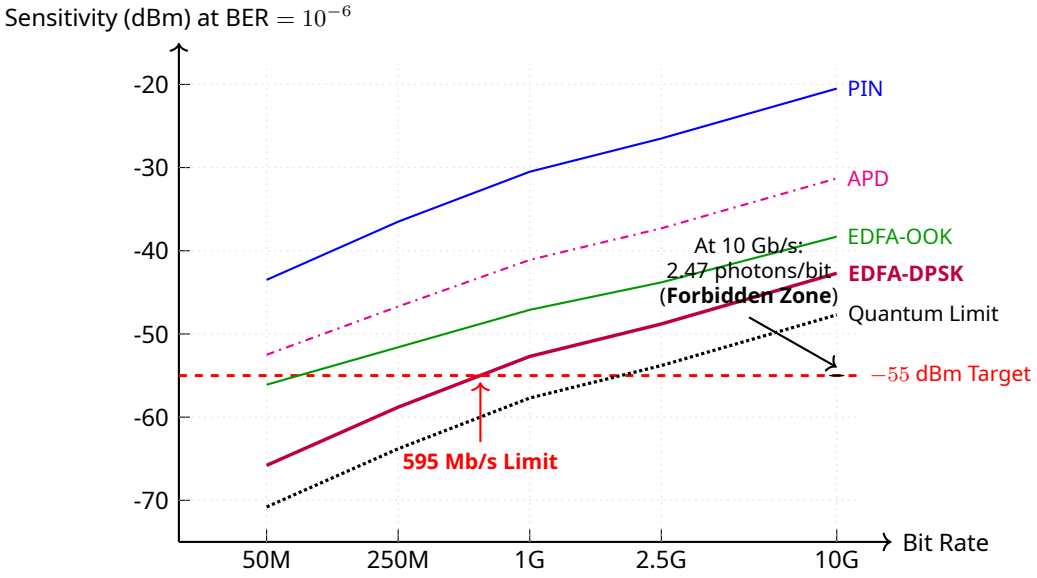


Figure 2: Pictorial representation of receiver sensitivity versus bit rate for PIN, APD, pre-amplified OOK, and pre-amplified DPSK, highlighting the 595 Mb/s crossover point and the unachievable -55 dBm zone at 10 Gb/s.

Link budgets for canonical space scenarios are summarized in Table 3, assuming $P_t = 1.0$ W and optical telescope apertures ranging from 0.10 m to 1.00 m without pointing loss.

4 Divergence Optimization Under Pointing Jitter

4.1 Fixed-Rate Links: Invariance to Jitter

Let S represent receiver sensitivity (in Watts) for a given fixed data rate. Link outage occurs when instantaneous received power falls below sensitivity ($P_{\text{rx}} < S$). Substituting Gaussian beam attenuation yields the outage condition:

$$\frac{K}{\theta^2} \exp\left(-\frac{2\theta_e^2}{\theta^2}\right) < S \iff \theta_e^2 > \frac{\theta^2}{2} \ln\left(\frac{K}{\theta^2 S}\right), \tag{12}$$

Table 3: Optical Space Link Budgets and Achievable Data Rates

Scenario	L (km)	θ (μrad)	D_r (m)	P_{rx} (dBm)	R_{DPSK}	R_{OOK}
LEO $\rightarrow$ Ground	1,000	15	0.40	-13.5	10.0G	10.0G
LEO $\leftrightarrow$ LEO	4,000	15	0.10	-34.6	10.0G	10.0G
GEO $\rightarrow$ Ground	38,000	10	1.00	-33.6	10.0G	10.0G
LEO $\rightarrow$ GEO	40,000	10	0.20	-45.0	5.91G	1.78G

defined for $K/\theta^2 > S$. Because orthogonal jitter components are Gaussian $\mathcal{N}(0, \sigma^2)$, the variable $u = \theta_e^2$ is exponentially distributed with parameter $\lambda_u = 1/(2\sigma^2)$:

$$f_u(u) = \frac{1}{2\sigma^2} \exp\left(-\frac{u}{2\sigma^2}\right), \qquad u \geq 0. \tag{13}$$

The outage probability is obtained by integrating over the outage tail:

$$\begin{aligned} P_{\text{out}}(\theta) &= \int_{\frac{\theta^2}{2}\ln\left(\frac{K}{\theta^2 S}\right)}^{\infty} \frac{1}{2\sigma^2} \exp\left(-\frac{u}{2\sigma^2}\right) du \\ &= \exp\left[-\frac{\theta^2}{4\sigma^2} \ln\left(\frac{K}{\theta^2 S}\right)\right]. \end{aligned} \tag{14}$$

To minimize outage probability $P_{\text{out}}(\theta)$, we maximize the exponent argument $g(\theta^2) = \theta^2 \ln[K/(\theta^2 S)]$. Setting $w = \theta^2$:

$$\frac{dg}{dw} = \ln\left(\frac{K}{wS}\right) + w \cdot \left(\frac{wS}{K}\right)\left(-\frac{K}{w^2 S}\right) = \ln\left(\frac{K}{wS}\right) - 1. \tag{15}$$

Equating the derivative to zero yields:

$$\ln\left(\frac{K}{w^* S}\right) = 1 \implies \frac{K}{(\theta^*)^2 S} = e. \tag{16}$$

Substituting $P_{\text{pk}}(\theta^*) = K/(\theta^*)^2$ establishes the optimal divergence geometry:

$$\theta^* = \sqrt{\frac{K}{e\,S}} \iff P_{\text{pk}}(\theta^*) = e \cdot S. \tag{17}$$

The corresponding minimum outage probability evaluates to:

$$P_{\text{out}}^* = \exp\left(-\frac{(\theta^*)^2}{4\sigma^2}\right). \tag{18}$$

Theorem 1 (Jitter Invariance): *For a fixed-rate free-space optical link operating over a Rayleigh pointing channel, the outage-optimal beam divergence θ^* is independent of the platform jitter magnitude σ. The optimal beam is uniquely achieved when on-axis peak received power exceeds receiver sensitivity by exactly e ($10 \log_{10} e \approx 4.34$ dB).*

Platform jitter determines the depth of the minimum outage, but does not alter where the minimum occurs. For a LEO–GEO link at 1 Gb/s ($S = -52.7$ dBm), $\theta^* = 14.7$ μrad across all jitter levels. This demonstrates that for fixed-rate inter-satellite links, variable beam divergence provides no geometric advantage; setting a static beam with a 4.34 dB margin is inherently optimal.

4.2 Rate-Adaptive Links: Linear Jitter Scaling

When transmission rate dynamically tracks link margin, the transmitter selects the maximum bit rate whose sensitivity S is guaranteed with probability $1 - P_{\text{out}}$. From (14), the guaranteed received power $P_g(\theta)$ satisfying $\Pr(P_{\text{rx}} \geq P_g) = 1 - P_{\text{out}}$ is:

$$P_g(\theta) = \frac{K}{\theta^2} \exp\left(\frac{4\sigma^2 \ln P_{\text{out}}}{\theta^2}\right). \tag{19}$$

Differentiating $P_g(\theta)$ with respect to θ and setting to zero yields the rate-adaptive optimum:

$$\theta_{\text{opt}} = \sigma\sqrt{-4 \ln P_{\text{out}}}, \qquad P_g(\theta_{\text{opt}}) = \frac{K}{e\,\theta_{\text{opt}}^2}. \tag{20}$$

In stark contrast to fixed-rate links, the optimal divergence for rate-adaptive links scales strictly linearly with jitter standard deviation σ. For $P_{\text{out}} = 10^{-3}$, $\theta_{\text{opt}} \approx 5.26\sigma$.

As shown in Table 4, as platform jitter doubles, the optimal beam must double in width, leading to a smooth ≈ 6 dB reduction in guaranteed power. Conversely, a static beam sized for quiet conditions ($\theta = 5.3$ μrad at $\sigma = 1.0$ μrad) suffers catastrophic link loss when jitter increases beyond 2.5 μrad.

Table 4: LEO–GEO Rate-Adaptive Throughput ($P_{\text{out}} = 10^{-3}$, DPSK)

Jitter σ (μrad)	θ_{opt} (μrad)	P_g (dBm)	Rate (Adaptive θ)	Rate (Fixed 5.3 μrad)
0.5	2.6	-37.8	$10{,}000$ Mb/s (capped)	$10{,}000$ Mb/s (capped)
1.0	5.3	-43.8	$7{,}870$ Mb/s	$7{,}870$ Mb/s
2.0	10.5	-49.8	$1{,}968$ Mb/s	392 Mb/s
3.0	15.8	-53.3	875 Mb/s	Link Lost
4.0	21.0	-55.8	492 Mb/s	Link Lost
5.0	26.3	-57.8	315 Mb/s	Link Lost

4.3 Turbulence Reintroduces Jitter Dependence

For trans-atmospheric downlinks (LEO to ground: $1{,}200$ km slant range, $P_t = 0.2$ W, $D_r = 0.1$ m, 10 Gb/s DPSK, $S = -42.7$ dBm), scintillation fades alter the optimization landscape. Jitter alone predicts an invariant optimum at $\theta^* = 27.6$ μrad.

Table 5 illustrates the resulting optimum divergences. Scintillation forces the optimal divergence to contract by a factor of $2\times$ to $9\times$, allowing higher on-axis power density to penetrate deep atmospheric fades. Furthermore, under moderate turbulence ($\sigma_R^2 = 1.0$), tripling the jitter from 1 μrad to 3 μrad shifts the optimum divergence from 3.4 μrad to 9.3 μrad. Thus, atmospheric turbulence restores jitter sensitivity even in fixed-rate links.

Table 5: Outage-Optimal Divergence with Gamma-Gamma Turbulence

Rytov Variance σ_R^2	$\sigma = 1.0$ μrad ($\theta_{\text{opt}}/P_{\text{out}}$)	$\sigma = 3.0$ μrad ($\theta_{\text{opt}}/P_{\text{out}}$)
0 (Analytic Jitter Only)	27.6 μrad / 1.0×10^{-83}	27.6 μrad / 6.4×10^{-10}
0.2 (Weak)	3–13 μrad / $< 5 \times 10^{-6}$	12.6 μrad / 1.6×10^{-4}
1.0 (Moderate)	3.4 μrad / 7.0×10^{-5}	9.3 μrad / 1.3×10^{-2}
3.0 (Strong)	3.2 μrad / 2.4×10^{-3}	8.6 μrad / 4.3×10^{-2}

5 Liquid-Lens Adaptive Terminal Evaluation

We evaluate dynamic beam control using a 60-second time-domain simulation of a LEO–GEO terminal modeled at a 1 kHz execution rate. The platform disturbance profile incorporates four operational phases:

- Quiet tracking (0–10 s, 20–30 s, 55–60 s): $\sigma = 0.6$ μrad.
- Reaction-wheel resonance (10–20 s): $\sigma = 2.5$ μrad.
- Thruster firing transient (30–34 s): $\sigma = 5.0$ μrad.
- Antenna slew tracking (45–55 s): $\sigma = 1.5$ μrad.

The adaptive terminal employs a four-state liquid lens ($\theta \in \{3, 6, 12, 24\}$ μrad). Commercial electrowetting and fluidic elastomeric lenses exhibit physical settling times between 5 and 15 ms for clear optical apertures up to 5 mm, well within our 100 ms control cycle. For major mechanical events (e.g., thruster firings), predictive feed-forward triggering commanded directly by the spacecraft Attitude Determination and Control System (ADCS) enables state switching prior to thruster plume activation, bypassing closed-loop estimator lag.

Every 100 ms, the controller computes the running variance of tracking sensor residuals over the preceding 200 ms, applies a $1.2\times$ safety factor, selects the divergence state maximizing guaranteed power P_g at $P_{\text{out}} = 10^{-3}$, and switches the transmission rate accordingly. Performance metrics across fixed and adaptive configurations are compiled in Table 6.

Table 6: Performance Comparison Over 60-Second Dynamic Disturbance Profile

Divergence	Fixed 1G Avail.	Quiet Rate	Disturbed Rate	Overall Rate
Fixed 3 μrad	91.6%	$9{,}717$ Mb/s	67 Mb/s	$5{,}832$ Mb/s
Fixed 6 μrad	97.4%	$9{,}842$ Mb/s	694 Mb/s	$6{,}160$ Mb/s
Fixed 12 μrad	99.2%	$3{,}685$ Mb/s	$1{,}264$ Mb/s	$2{,}710$ Mb/s
Fixed 24 μrad	82.0%	996 Mb/s	680 Mb/s	869 Mb/s
Adaptive Lens	N/A (Adaptive)	$9{,}850$ Mb/s	$1{,}357$ Mb/s	$6{,}431$ Mb/s

The simulation highlights two distinct operational behaviors:

1. *Fixed-Rate Links:* The optimal static beam is 12 μrad (99.2% availability), matching the theoretical jitter-invariant optimum $\theta^* = 14.7$ μrad. The liquid lens provides negligible improvement here.

2. *Rate-Adaptive Links:* No single static beam optimizes both regimes. The 6 μrad beam achieves high quiet throughput ($9{,}842$ Mb/s) but drops to 694 Mb/s during disturbances; the 12 μrad beam prevents outages but limits quiet throughput to $3{,}685$ Mb/s. The adaptive liquid lens matches the best beam in each phase (3 μrad when quiet, 12–24 μrad when disturbed), delivering $1{,}357$ Mb/s during disturbances—a 95% **throughput gain** over the static 6 μrad beam—while preserving full multi-gigabit throughput during quiet intervals.

Preprint submitted to IEEE for possible publication. Copyright may be transferred without notice.

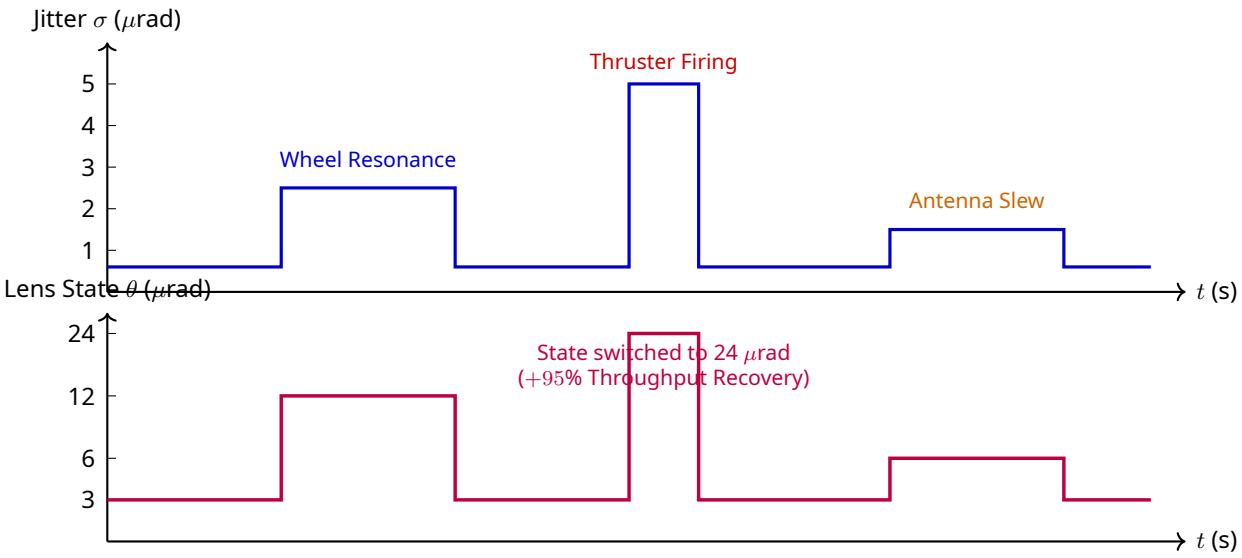


Figure 3: Dynamic time-domain controller simulation over 60 seconds: (top) spacecraft attitude pointing jitter disturbance profile $\sigma(t)$; (bottom) discrete liquid-lens divergence states selected to maximize guaranteed throughput.

6 Discussion and Engineering Rules

These findings provide clear engineering guidelines for space optical terminal design:

- **Sensitivity Benchmarks and Pre-FEC Thresholds:** Optical receiver sensitivity should be specified in photons per bit rather than flat power levels across multi-gigabit bands. A sensitivity of ≈ 40 photons/bit is realistic for uncoded pre-amplified balanced DPSK, improving to ≈ 19.5 photons/bit with high-gain soft-decision LDPC. Uniform agency targets of -55 dBm across 50 Mb/s to 10 Gb/s violate the quantum limit above 1.88 Gb/s (and above 3.5 Gb/s with advanced FEC), remaining unachievable in practical receivers at 10 Gb/s.
- **Fixed-Rate Inter-Satellite Links:** Dynamic divergence control is unnecessary on fixed-rate inter-satellite links. Terminals should employ a static beam designed so that peak received power exceeds sensitivity by 4.34 dB ($P_{\text{pk}} = e \cdot S$); pointing jitter then dictates outage probability, but does not shift the optimum beam geometry.
- **Rate-Adaptive and Downlink Systems:** Liquid-lens divergence control is highly advantageous for rate-adaptive links and ground downlinks experiencing turbulence. A four-state liquid lens provides nearly all the throughput gains of continuous beam adaptation, offering significant resilience during mechanical disturbances.
- **Aperture Averaging Considerations:** While our terrestrial downlink simulations model a point-receiver baseline, ground stations utilizing collection apertures $D_r \geq 0.4$ m will benefit from spatial aperture averaging. This suppresses the effective scintillation index σ_I^2, narrowing the optimal beam divergence closer to the jitter-only optimum.

7 Conclusion

This study defines fundamental sensitivity and beam divergence boundaries for space laser communications. We demonstrated that agency specifications requiring -55 dBm

sensitivity up to 10 Gb/s violate the quantum limit, establishing that practical pre-amplified DPSK systems can achieve -55 dBm only up to ≈ 600 Mb/s. Furthermore, we proved that the outage-optimal beam divergence for fixed-rate inter-satellite links is invariant to pointing jitter magnitude, requiring only a static beam tuned 4.34 dB above sensitivity. Conversely, for rate-adaptive links and trans-atmospheric channels, dynamic liquid-lens divergence control provides substantial operational advantages, yielding a 95% throughput improvement during spacecraft disturbance transients.

References

[1] K. Böhmer, M. Gregory, F. Heine, H. Kämpfner, R. Lange, M. Lutzer, and R. Meyer, "Laser communication terminals for the European Data Relay System," in *Proc. SPIE 8246*, p. 82460D, 2012.

[2] H. Kaushal and G. Kaddoum, "Optical communication in space: Challenges and mitigation techniques," *IEEE Commun. Surveys Tuts.*, vol. 19, no. 1, pp. 57–96, 2017.

[3] ISRO Capacity Building and Public Outreach, "RESPOND Basket 2025," Research Problem RES-SAC-2025-007, Space Applications Centre, Dec. 2025.

[4] D. O. Caplan, "Laser communication transmitter and receiver design," *J. Opt. Fiber Commun. Rep.*, vol. 4, pp. 225–362, 2007.

[5] C.-C. Chen and C. S. Gardner, "Impact of random pointing and tracking errors on the design of coherent and incoherent optical intersatellite communication links," *IEEE Trans. Commun.*, vol. 37, no. 3, pp. 252–260, Mar. 1989.

[6] M. Toyoshima, T. Jono, K. Nakagawa, and A. Yamamoto, "Optimum divergence angle of a Gaussian beam wave in the presence of random jitter in free-space laser communication systems," *J. Opt. Soc. Am. A*, vol. 19, no. 3, pp. 567–571, Mar. 2002.

[7] A. A. Farid and S. Hranilovic, "Outage capacity optimization for free-space optical links with pointing errors," *J. Lightw. Technol.*, vol. 25, no. 7, pp. 1702–1710, Jul. 2007.

[8] Z. Xue, B. Qi, G. Ren, and Z. Xie, "Design of optimum beam divergence angle for intersatellite optical communication systems with pointing errors," *Laser Optoelectron. Prog.*, vol. 52, no. 7, p. 070602, 2015.

[9] S. Arnon and N. S. Kopeika, "Possible solutions to mitigate vibration effects in laser intersatellite links," in *Proc. SPIE 4489*, pp. 202–207, Jan. 2002.

[10] V. V. Mai and H. Kim, "Beaconless PAT and adaptive beam control using variable focus lens for free-space optical communication systems," *APL Photonics*, vol. 6, no. 2, p. 020801, Feb. 2021.

[11] K. Lee, V. Mai, and H. Kim, "Dynamic adaptive beam control system using variable focus lenses for laser inter-satellite link," *IEEE Photon. J.*, vol. 14, no. 4, Art. no. 7903808, Aug. 2022.

[12] F. A. Fogle, "Liquid lens beam steering and environmental testing for the miniature optical steered antenna for inter-satellite communication," S.M. thesis, Dept. Aeronaut. Astronaut., Massachusetts Inst. Technol., Cambridge, MA, USA, 2020.

Preprint submitted to IEEE for possible publication. Copyright may be transferred without notice.